A FLUID MODEL FOR MULTIPLE-MIRROR AXIAL PLASMA FLOW

PART I —— PRELIMINARIES

by

R. Bravenec

Memorandum No. UCB/ERL M79/49

11 June 1979

ELECTRONICS RESEARCH LABORATORY

College of Engineering
University of California, Berkeley
94720

A FLUID MODEL FOR MULTIPLE-MIRROR AXIAL PLASMA FLOW

PART I — PRELIMINARIES*

R. Bravenec

Department of Electrical Engineering and Computer Science

&

Electronics Research Laboratory

University of California

Berkeley CA 94720

ABSTRACT

The fluid equations are solved for a straight magnetic field and a single mirror under the assumption of a steady-state, one-dimensional, isothermal flow. The latter assumption is found to be a poor one during supersonic, shocked flow; otherwise, it is acceptable. Flow through a magnetic mirror is studied as a function of the relative viscosity of the plasma and compared to fluid flow through a converging-diverging nozzle. Finally, applications to multiple-mirror flow are discussed.

---

*Sponsored by Department of Energy Grant No. DE-AS03-76F00034-PA# DE-ATOE-76ET53059.

A FLUID MODEL FOR MULTIPLE-MIRROR AXIAL PLASMA FLOW

PART I — PRELIMINARIES

I. INTRODUCTION

This report lays the foundation for studying multiple-mirror axial plasma flow via a fluid model. The fluid equations are solved for a uniform magnetic field and for a converging-diverging field (a magnetic mirror). The latter configuration is of interest because a multiple-mirror device is a succession of single mirrors. Our interest in a uniform field is in studying the basic characteristics of the equations and their solutions.

Frequently we will compare the plasma flow along the magnetic field to actual fluid flow through pipes of varying cross-section. The similarity is clear after making the following assumptions: the plasma-vacuum interface is sharp and the plasma is of low β, so that the magnetic field is considered a known function of z. Through conservation of magnetic flux the plasma cross-section A is also known.[1] Thus we may compare the plasma flow to that of a fluid flowing through a pipe of cross-section $A(z)$.

Throughout this report the flow is assumed steady, one-dimensional and isothermal. A steady-state results from an arbitrary plasma source at the system origin and a sink at the exit. Radial motion

---

[1]For high β, $A(z)$ is not so simply related to the vacuum magnetic field but must be solved for via pressure balance, as in Taylor and Wesson [1].

is neglected by making a "long, thin approximation" with B_z large enough to prevent any significant radial diffusion. Finally, isothermy originates from a large electron thermal conductivity which maintains $T_e(z) = T$, a constant. This is communicated to the ions via ion-electron collisions on the time scale $\tau_{ie}^{\varepsilon} \sim \tau_{ie} \sim \sqrt{m_i/m_e}\,\tau_{ii}$, where the superscript ε denotes an *energy* exchange time, and where τ_{ie} and τ_{ii} are the ion-electron and ion-ion *scattering* times, respectively. (See Trubnikov [2].) Thus, for isothermal ions we require that $\tau_{ie} \ll \tau_s$, where τ_s is the time for a fluid element to traverse the scale length of inhomogeneity of the fluid ℓ_s. All other electron effects are ignored in the analysis which follows. With this assumption the similarity between the plasma flow and that of a viscous fluid is even more pronounced. In fact, the equation of motion used here differs from the Navier-Stokes Equation only in the form of the viscosity term. In a straight system they are identical.

Section II presents the fluid equations and the derivation of a second-order ODE for the fluid velocity. This equation is cast in dimensionless form to select out the important parameters of the problem and becomes the basis for most of this report. Section III presents the analytical solutions of this equation for a uniform magnetic field. In Sec. IV an analytical solution neglecting viscosity is obtained for a magnetic mirror; however, this solution does not give transonic solutions (transitions from subsonic to supersonic flow, or vice versa). The transonic case is discussed qualitatively, drawing heavily from Shapiro [3]. Finally, the mirror-flow problem, including

viscosity, is solved numerically and the results compared to the inviscid case. Section V ummarizes the results and discusses the applications to multiple-mirror flow.

II. THE FLUID EQUATIONS

The following are taken directly from Dawson and Uman [4] ignoring the electrostatic potential and setting $\partial/\partial t = 0$.

ION EQUATION OF MOTION

$$nm_i v \frac{dv}{dz} = - \frac{d}{dz}(nT_{\parallel}^i) + \frac{1}{A}\frac{d}{dz}\left(nAm_i \nu_i \frac{dv}{dz}\right) + n(T_{\perp}^i - T_{\parallel}^i)\frac{1}{A}\frac{dA}{dz} \qquad (1a)$$

CONTINUITY EQUATION

$$\frac{d}{dz}(nAv) = 0 \qquad (1b)$$

PERPENDICULAR ION TEMPERATURE

$$v \frac{dT_{\perp}^i}{dz} = - \frac{T_{\perp}^i - T_{\parallel}^i}{\tau_{ii}} + \frac{2\nu_i m_i}{3}\left(\frac{dv}{dz}\right)^2 - \frac{T_{\perp}^i}{A} v \frac{dA}{dz}$$

$$+ \frac{1}{\tau_{ei}}\frac{m_e}{m_i}\left[\frac{2}{3}(T_{\perp}^e - T_{\perp}^i) + \frac{1}{3}(T_{\parallel}^e - T_{\parallel}^i)\right]$$

$$+ \frac{1}{3nA}\frac{d}{dz}\left[nA\kappa_i \frac{d}{dz}(T_{\parallel}^i + 2T_{\perp}^i)\right] \qquad (1c)$$

PARALLEL ION TEMPERATURE

$$v \frac{dT_{\parallel}^i}{dz} = \frac{2(T_{\perp}^i - T_{\parallel}^i)}{\tau_{ii}} + \frac{2\nu_i m_i}{3}\left(\frac{dv}{dz}\right)^2 - 2T_{\parallel}^i \frac{dv}{dz}$$

$$+ \frac{1}{\tau_{ei}}\frac{m_e}{m_i}\left[\frac{2}{3}(T_{\perp}^e - T_{\perp}^i) + \frac{1}{3}(T_{\parallel}^e - T_{\parallel}^i)\right]$$

$$+ \frac{1}{3nA}\frac{d}{dz}\left[nA\kappa_i \frac{d}{dz}(T_{\parallel}^i + 2T_{\perp}^i)\right] \qquad (1d)$$

FLUX CONSERVATION

$$A = A_o \frac{B_o}{B} \qquad (1e)$$

In the above, n is the ion density (assumed equal to the electron density), A is the plasma cross-section, v is the z-component of the flow velocity (same for ions and electrons), $T_{\parallel}^{(e,i)}$ and $T_{\perp}^{(e,i)}$ are the electron and ion temperatures (in energy units) respectively parallel and perpendicular to the magnetic field, m_i and m_e are the ion and electron masses, ν_i is the ion bulk viscosity, τ_{ii} and τ_{ei} are the ion-ion and electron-ion collision times, and κ_i is the ion thermal conductivity.[2] The reader is referred to Dawson and Uman for a thorough discussion of these equations.

Although we ultimately set $T_{\perp}^i = T_{\parallel}^i = T$, Eqs. (1c) and (1d) are included to evaluate the last term of Eq. (1a). We cannot simply set $T_{\perp}^i = T_{\parallel}^i$ here since this term is found to be of the same order as the bulk viscosity term. Setting

$$\frac{dT_{\perp}^i}{dz} = \frac{dT_{\parallel}^i}{dz} = 0$$

in Eqs. (1c) and (1d), subtracting them from each other and then setting $T_{\perp}^i = T_{\parallel}^i = T$ thereafter (except in the difference $T_{\perp}^i - T_{\parallel}^i$), we obtain

---

[2]Throughout this report all quantities subscripted with a zero are evaluated at $z = 0$, i.e., $A_o \equiv A(0)$, $B_o \equiv B(0)$, etc.

$$T_{\perp}^{i} - T_{\parallel}^{i} \simeq \frac{1}{3}\tau_{ii}\, T\, \frac{A}{v}\, \frac{d}{dz}\left(\frac{v^2}{A}\right) \tag{2}$$

Thus, the temperature difference is proportional to the small quantity τ_{ii}, as is the ion bulk viscosity

$$\nu_i = \frac{\alpha}{m_i}\tau_{ii}\, T \tag{3}$$

(α of order unity). Substituting Eqs. (2) and (3) into Eq. (1a), we have

$$v\frac{dv}{dz} = \frac{-1}{m_i n}\frac{d(nT)}{dz} + \frac{\alpha}{m_i nA}\frac{d}{dz}\left(\tau_{ii} TnA\frac{dv}{dz}\right) + \frac{1}{3}\frac{\tau_{ii} T}{m_i v}\frac{dA}{dz}\frac{d}{dz}\left(\frac{v^2}{A}\right) \tag{4}$$

Next we define the following dimensionless quantities

$$\eta \equiv \frac{n}{n_o}\ ,\quad \nu \equiv \frac{v}{v_o}\ ,\quad a \equiv \frac{A}{A_o}\ ,\quad \zeta \equiv \frac{z}{\ell_c}\ ,\quad M \equiv \frac{v}{v_s} = M_o\nu \tag{5}$$

Here ℓ_c is an appropriate reference length in the problem, i.e., the cell length of a multiple mirror, and $v_s \equiv \sqrt{T/m_i}$ is the sound speed (also the ion thermal speed). Substituting into Eq. (4) and using the relation $\tau_{ii} = \lambda/v_s \propto T^{3/2}/n$, where λ is the ion-ion mean-free-path, we obtain

$$\nu\frac{d\nu}{d\zeta} = \frac{-1}{M_o^2}\frac{1}{\eta}\frac{d\eta}{d\zeta} + \frac{\lambda_o}{\ell_c}\frac{\alpha}{M_o}\frac{1}{\eta a}\frac{d}{d\zeta}\left(a\frac{d\nu}{d\zeta}\right) + \frac{1}{3}\frac{\lambda_o}{\ell_c}\frac{1}{M_o}\frac{1}{\eta\nu}\frac{da}{d\zeta}\frac{d}{d\zeta}\left(\frac{\nu^2}{a}\right) \tag{6a}$$

The continuity equation becomes simply

$$\eta a\nu = 1 \tag{6b}$$

Using Eq. (6b) to eliminate η, Eq. (6a) becomes

$$v\frac{dv}{d\zeta} - \frac{1}{M_o^2}\frac{1}{av}\frac{d(av)}{d\zeta} = \frac{\lambda_o}{\ell_c}\frac{1}{M_o}\left[\alpha v\frac{d}{d\zeta}\left(a\frac{dv}{d\zeta}\right) + \frac{a}{3}\frac{da}{d\zeta}\frac{d}{d\zeta}\left(\frac{v^2}{a}\right)\right] \quad (7)$$

Equation (7) is a second-order ODE for the normalized flow velocity v in terms of the known area function $a(\zeta)$ and the two parameters λ_o/ℓ_c and M_o, hereafter referred to as the "flow equation". Its solution is completely determined given the two boundary conditions $v(0)$ and $dv/d\zeta(0)$ (or $v(0)$ and $v(L/\ell_c)$), where L is the system length). The first of each set is trivial since by definition $v(0) \equiv 1$. (The boundary condition $v(0)$ makes its appearance through the parameter M_o.) Recall that the terms on the left-hand side represent the ion inertia and scalar pressure, respectively. The term on the right represents the combined effects of pressure anisotropy and will hereafter be referred to as simply the "viscosity term." For $v \sim dv/d\zeta \sim d^2v/d\zeta^2 \sim O(1)$, the relative order of each term is easily seen to be

$$\text{inertia} : \text{pressure} : \text{viscosity} = M_o^2 : 1 : \frac{\lambda_o}{\ell_c} M_o$$

Thus for $M_o, \lambda_o/\ell_c \ll 1$ the pressure term is dominant. However, for $v \simeq 1/M_o$ so that $M \simeq 1$, the ordering becomes $1 : 1 : (\lambda_o/\ell_c)(1/M_o)$ so that all terms may be comparable.

For future reference it is useful to rewrite the condition for uniform ion temperature in terms of our dimensionless variables. First it can be shown that $\tau_s = (1/M)(\ell_s/\ell_c)(\ell_c/\lambda)\tau_{ii}$. Since $\lambda \propto 1/n$ this can be written $\tau_s = (1/M)(\ell_c/\lambda_o)(\ell_s/\ell_c)(\tau_{ii}/\eta)$. Hence,

the condition for isothermal ions becomes

$$\frac{\lambda_o}{\ell_c}\frac{\ell_c}{\ell_s}\frac{M}{\eta} \ll \sqrt{\frac{m_e}{m_i}} \tag{8}$$

Finally, we should note that Eq. (4) differs from that used by Miller [5], who derives the force equation directly from Braginskii [6]. The differences, which as of yet have not been resolved, lie in the explicit form of the viscosity term. Since this term is usually small, we will not overly concern ourselves with this discrepancy.

III. FLOW ALONG A UNIFORM MAGNETIC FIELD

Setting $a = 1$ in Eq. (7) we have

$$\nu \frac{d\nu}{d\zeta} - \frac{1}{M_o^2} \frac{1}{\nu} \frac{d\nu}{d\zeta} = \frac{\lambda_o}{\ell_c} \frac{\alpha\nu}{M_o} \frac{d^2\nu}{d\zeta^2} \tag{9}$$

Notice that the temperature anisotropy term has dropped out, leaving us with the Navier-Stokes Equation. Dividing by ν and integrating once, there results

$$\nu - 1 + \frac{1}{M_o^2}\left(\frac{1}{\nu} - 1\right) = \frac{\lambda_o}{\ell_c} \frac{\alpha}{M_o} \left(\frac{d\nu}{d\zeta} - \nu_o'\right)$$

where

$$\nu_o' \equiv \frac{d\nu}{d\zeta}(0)$$

Solving for $d\nu/d\zeta$, we obtain

$$\frac{d\nu}{d\zeta} = \frac{\lambda_o}{\ell_c} \frac{1}{\alpha}\left[M_o(\nu - 1) + \frac{1}{M_o}\left(\frac{1}{\nu} - 1\right)\right] + \nu_o' \tag{10}$$

This equation can be integrated by first separating variables. For $\nu_o' \neq 0$

$$\frac{\nu d\nu}{M_o\nu^2 - \left(M_o + \frac{1}{M_o} - \frac{\lambda_o}{\ell_c}\alpha\nu_o'\right)\nu + \frac{1}{M_o}} = \frac{\ell_c}{\lambda_o} \frac{d\zeta}{\alpha} \tag{11}$$

The results of the integration depend on whether $M_o < 1$ or $M_o > 1$. For

$$|\nu'_o| \ll \frac{\ell_c}{\lambda_o} \frac{1}{2\alpha} \frac{\left(M_o^2 - 1\right)^2}{M_o(M_o^2 + 1)}$$

the expressions are particularly simple[3]

$$\zeta = \frac{\lambda_o}{\ell_c} \frac{\alpha}{1 - M_o^2} \left[\frac{1}{M_o} \ln\left(\frac{1/M_o^2 - \nu}{1/M_o^2 - 1} \right) - M_o \ln\left(\frac{1 + \mu'_o - \nu}{\mu'_o} \right) \right] , \quad M_o < 1 \qquad (12a)$$

$$\zeta = \frac{\lambda_o}{\ell_c} \frac{\alpha}{M_o^2 - 1} \left[M_o \ln\left(\frac{1 + \mu'_o - \nu}{\mu'_o} \right) - \frac{1}{M_o} \ln\left(\frac{\nu - 1/M_o^2}{1 - 1/M_o^2} \right) \right] , \quad M_o > 1 \qquad (12b)$$

where

$$\mu'_o \equiv \frac{\lambda_o}{\ell_c} \frac{\alpha M_o}{1 - M_o^2} \nu'_o \qquad (12c)$$

There are two distinct profiles given by each of Eqs. (12), depending on the sign of ν'_o. For $\nu'_o < 0$, Eq. (12a) gives the same profile as (12b) except shifted in ζ. Choosing $\nu'_o > 0$ in Eq. (12b) leads to an entirely unphysical profile in which the velocity increases without bound. Thus, we are left with the two cases $M_o < 1$, $\nu'_o > 0$ and $M_o > 1$, $\nu'_o < 0$.

---

[3]This inequality is imposed only to obtain the simple forms of Eqs. (12), and only restricts our placement of the origin relative to the profiles.

As an example of the former, consider the choices $M_o = 0.5$, $\nu_0' = 0.01$, $\alpha = 1$ for which Eq. (12a) gives the profiles shown in Fig. 1(a). Here λ_o/ℓ_c is set to one so that the units of ζ are mean-free-paths. Superimposed on the curve $M = M_o\nu$ is that of η, obtained from the continuity relation $\eta\nu = 1$. The most obvious feature of the curves is that $M \to 0$ and $\eta \to \infty$ at a point ζ_{min} to the left of the origin, where

$$\zeta_{min} = \frac{\alpha}{M_o(1 - M_o^2)} \ln \left[\frac{\left(\mu_o'\right)^{M_o^2}}{1 - M_o^2} \right]$$

Although we have imposed an upper limit on $|\nu_o'|$ to obtain Eqs. (12), solutions certainly exist for ν_o' large. For example, shifting the curves of Fig. 1(a) to the right by an amount less than $|\zeta_{min}|$ represents such a solution. The resulting flow is then characterized by an acceleration and pressure drop within a few mean-free-paths into the system. Whatever the source of the initial velocity gradient, the important point here is that bulk viscosity does not lead to an increasingly accelerating flow, as is the case during fluid flow through pipes with wall friction [3]. Instead, it simply smooths out the initial gradients, causing the profiles to asymptote to steady values. Note that for $\nu_o' = 0$, M_o arbitrary, Eq. (9) has the trivial solution $\eta = \nu = 1$, which may be easily seen from Eq. (10). We have just shown that the equations have a preference for such a uniform solution; thus we conclude that the imposition of $\nu_o' > 0$ does not represent an easily realizable physical system. This conclusion will be applied in the next section on flow through a magnetic mirror.

An example of the case $M_o > 1$, $\nu'_o < 0$ is presented in Fig. 1(b) for $M_o = 2.0$, $\nu'_o = -0.01$, $\alpha = 1$. As required by basic fluid theory [3], the velocity decreases and the density increases during viscous supersonic flow. These profiles represent a shock front, resulting in a transition to subsonic flow ($M \simeq 0.5$) over a distance of about four mean-free-paths. Referring back to Eq. (12b), we see that in general the two asymptotes of $\nu(\zeta)$ are $\nu_{max} \simeq 1$ and $\nu_{min} \simeq 1/M_o^2$, such that the shock strength is $\nu_{max}/\nu_{min} = M_o^2$. In a frame with $\lambda_o/\ell_c \ll 1$, Eq. (12b) predicts an almost discontinuous profile. This is expected since the shock thickness depends on the magnitude of the viscosity term which in turn is proportional to λ_o/ℓ_c . Furthermore, on either side of the shock $d\nu/d\zeta$ is very small. Thus, for a fixed value of M_o , varying ν'_o within the range

$$0 < |\nu'_o| < \frac{\ell_c}{\lambda_o} \frac{1}{2\alpha} \frac{(M_o^2 - 1)^2}{M_o (M_o^2 + 1)}$$

has the effect of shifting the shock along ζ . (Letting $\nu'_o \to 0$ drives the shock toward $+\infty$.) This behavior will reappear in the following section on mirror flow.

Before continuing, we should realize that the previous results are not to be interpreted too literally. First of all we have no justification in accepting solutions which vary significantly over a few mean-free-paths. This is a direct consequence of the limitations of the fluid theory. Thus, we should be wary of the "boundary-layer effect" predicted by Eq. (12a) or the details of the shock structure of Eq. (12b). As to

the latter, however, we are justified in accepting the values attained by the profiles downstream of the shock. This is because the equations conserve such quantities as mass and momentum flux [3]. That is, the shock strength predicted by Eq. (12b) is correct under the assumption of isothermy. However, as mentioned in the Introduction, this assumption is valid only for $T_e(z) = T$, a constant, and $\tau_{ie} \ll \tau_s$. Referring to Eq. (8) with $\ell_s \sim \lambda_o$, $M \sim 1$ and $\eta \sim 1$, the latter condition is badly violated and isothermy is a poor assumption. We will not let this deter us, however, since our ultimate intention is not to study shock fronts but subsonic, shock-free flow through a multiple-mirror, for which isothermy is a fair assumption. If desired we may imagine the temperature maintained uniform across the shock by some external means.

IV. FLOW THROUGH A MAGNETIC MIRROR

For this section and the remainder of this report we use the area function

$$a(\zeta) = \frac{R+1}{2R} + \frac{R-1}{2R} \cos 2\pi\zeta \tag{13}$$

where $R \equiv B_{max}/B_{min}$, the mirror ratio. This function is sketched for $R = 2$ in Fig. 2. Substituting Eq. (13) into Eq. (7) results in an expression that can be solved easily only in the limit $\lambda_o/\ell_c = 0$. In this case, Eq. (7) becomes

$$\nu \frac{d\nu}{d\zeta} = \frac{1}{M_o^2} \frac{d \ln a\nu}{d\zeta}$$

Solving for $d\nu/d\zeta$,

$$\frac{d\nu}{d\zeta} = \frac{1}{a} \frac{da}{d\zeta} \frac{\nu}{(M_o\nu)^2 - 1} \tag{14}$$

This can be integrated to yield

$$\nu^2 - \frac{2}{M_o^2} \ln a\nu = 1 \tag{15a}$$

Using Eq. (6b) we can write this in terms of η

$$a^2\eta^2 \left(1 - \frac{2}{M_o^2} \ln \eta\right) = 1 \tag{15b}$$

Eqs. (15) are sketched in Fig. 3 for $R = 2$ and the two choices (a) $M_o = 0.25$ and (b) $M_o = 2.0$. As expected the subsonic solution is characterized by a density minimum and a velocity maximum in the mirror throat, and the supersonic solution by just the opposite. Notice further that for $a(\zeta)$ periodic with period unity the solutions are similarly periodic. This means that there is no overall density (pressure) drop across a succession of such mirrors. We will return to this point in the final section. Referring to Eq. (14), the solution becomes singular at $\nu = 1/M_o$ $(M=1)$, preventing a transonic solution.

We now discuss qualitatively the family of solutions, both subsonic and transonic, for an inviscid fluid flowing through a converging-diverging nozzle. We imagine being given the inlet pressure p_o and investigating the flow as a function of the exit pressure p_1. References are repeatedly made to Fig. 4, taken from Shapiro, p. 140, which is for adiabatic flow of a perfect gas. Initially, entirely subsonic flow results when p_1 is reduced below p_o, as in Fig. 3(a). This is shown by case (a) of Fig. 4. Lowering p_1 further, state (b) is eventually reached, where the velocity in the throat has reached $M = 1$ (sonic flow), but the flow downstream is still subsonic. The flow is now choked, meaning that no further reduction in p_1 affects the flow upstream of the throat or increases the fluid flux. Between cases (b) and (f) there exist no values of p_1 that result in smooth shock-free flow. Case (f) corresponds to a unique value of p_1 for which shock-free supersonic flow does exist in the diverging section. Cases (c) and (d) represent shock fronts involving abrupt transitions from supersonic to subsonic flow. As p_1 is reduced from that of case (b) the shock is seen to progressively

move down the nozzle. The flow approaches that of case (d), in which the shock occurs at the exit. Except for case (f), further reduction of the exit pressure results in oblique shocks outside the nozzle, as represented by cases (e) and (g). These effects are two-dimensional and cannot be treated in our simple theory.

The flow characterized in Fig. 4 is that of an adiabatic, inviscid fluid. We wish now to investigate the effects of isothermy and viscosity. For $\lambda_o/\ell_c \ll 1$ we expect Fig. 4 to be qualitatively duplicated since the viscosity term of Eq. (7) is then small. The slight amount of viscosity simply gives structure to the shock fronts (Fig. 1(b)) so that no singularities occur in the flow equation. Furthermore we expect that our imposition of constant temperature only affects the magnitude of variation of ν and η, but not the general behavior characterized in Fig. 4.

The flow equation (7) is solved numerically using an integrating routine devised by Gear and Hindmarsh [7]. The program requires a system of first-order ODE's necessitating the definition of a new variable

$$\nu' \equiv \frac{d\nu}{d\zeta} \tag{16a}$$

Eq. (7) then becomes

$$\frac{d\nu'}{d\zeta} = \frac{1}{a}\frac{da}{d\zeta}\nu\left[\frac{1}{3\alpha}\frac{1}{a}\frac{da}{d\zeta} - \left(1+\frac{2}{3\alpha}\right)\frac{\nu'}{\nu}\right] + \frac{1}{\alpha}\frac{\ell_c}{\lambda_o}\frac{1}{a\nu}\left[\left(M_o\nu - \frac{1}{M_o\nu}\right)\nu' - \frac{1}{M_o}\frac{1}{a}\frac{da}{d\zeta}\right] \tag{16b}$$

In the following, α is set to 0.96 [6]. The routine further requires all boundary conditions to be given at $\zeta = 0$, namely $\nu(0)$ and $\nu'(0)$. (As mentioned earlier, we have defined $\nu(0) = 1$ so that $\nu(0)$ appears through the parameter M_o.) Thus, given a value for λ_o/ℓ_c, the solution to the system of Eqs. (16) is completely determined by the set M_o and $\nu'_o \equiv \nu'(0)$.

To generate curves similar to those of Fig. 4, λ_o/ℓ_c is set to 0.01, so that the fluid is nearly inviscid. From the findings of the last section, ν'_o is set to zero since the plasma initially sees a straight system $da/d\zeta(0) = 0$. Two cases of entirely subsonic flow are presented in Fig. 5 for $M_o = 0.25$ and $M_o = 0.3$. We immediately note that the small amount of viscosity shifts the velocity maximum and density minimum into the divergent section of the mirror. As M_o is increased to duplicate case (b) of Fig. 4, a value is reached for which sonic flow first occurs at a point slightly beyond the mirror throat. This situation is represented by the case labeled $M_o = 0.3175$. As M_o is increased further, the flow becomes supersonic over a short distance with a subsequent smooth transition back to subsonic flow. This behavior is interpreted as a weak shock developing in the divergent section of the mirror. As M_0 is increased still further, approaching sonic flow in the throat, the shock front grows in amplitude, steepens, and moves downstream. Curves for which $M \simeq 1$ in the throat[4] are presented in Fig. 5, corresponding

---

[4]The value of M in the mirror throat is simply estimated from the curves. Hence, there is a small uncertainty involved in the actual value.

to $M_o = 0.3225$.[5] An interesting phenomenon occurs if M_o is chosen just slightly larger so that M is barely greater than unity in the throat — the solution for ν diverges, indicating an unphysical solution. An example is the case labeled $M_o = 0.325$. Thus, the numerical solutions preserve the phenomenon of choking — no physical steady-state solutions for M_o larger than a critical value. Furthermore, it appears that choking occurs for $M = 1$ in the throat even during isothermal viscous flow.

In order to proceed further and generate curves analogous to cases (b) through (f) of Fig. 4, we begin the integration at $\zeta = 0.5$ (in the mirror throat) where we may accurately impose the condition $M = 1$. This leaves only the quantity $\nu'(.5)$ with which to determine the flow. As argued in the inviscid fluid case, the flow upstream of the throat is unaffected by reducing the exit pressure. Thus, in the following cases the profiles upstream of the throat are those for critical flow. It should be recalled that the relevant physical parameter that is being varied here is the exit pressure (density) via the boundary condition $\nu'(.5)$. Thus, only those values of $\nu'(.5)$ giving $\eta(1.0) \leq \eta_{crit}(1.0)$ are valid. This condition translates to $\nu'(.5) \geq \nu'_{crit}(.5)$. It is found that there exists a maximum value of $\nu'(.5)$ above which the solution diverges. This valve, which we will denote by $\nu'_{max}(.5)$, corresponds to the instance of smooth, shock-free supersonic flow, as in case (f) of Fig. 4. Furthermore $\nu'_{max}(.5)$ is found to be only slightly larger than $\nu'_{crit}(.5)$, leaving us only the restricted range $\nu'_{crit}(.5) \leq \nu'(.5) \leq \nu'_{max}(.5)$

[5] This case is hereafter referred to as "critical flow". In the following discussion its solutions η and ν are subscripted with "crit".

with which to work. In order to generate a shock front and move it downstream, $v'(.5)$ must be chosen very near $v'_{max}(.5)$. To accomplish this, the program was modified to search for that value of $v'(.5)$ which yields a specified value of $\eta(1.0)$, the physical boundary condition. The results for three choices of $\eta(1.0)$ are presented in Fig. 5, labeled $\eta(1.0) = 0.85$, 0.65, and 0.2. As evident from the curves, the differences between their values of $v'(.5)$ are unnoticable. The case $\eta(1.0) = 0.20$ corresponds to all but the "tail" of the shock having moved out the system.

Thus, we have seen that the boundary condition on $dv/d\zeta$ is only important in generating the flow profiles downstream of the throat in a choked system. Otherwise M_0 has by far the dominant role. We have also seen that the effect of $v'(.5)$ is the same as in our previous study of shocks in a straight field — that is, it shifts the location of the shock. Finally, we should mention that isothermy is a fair assumption only for the case labeled $M_0 = 0.25$. That this is so can be seen using Eq. (8) with $\lambda_o/\ell_c = 0.01$, $\ell_s/\ell_c \simeq \frac{1}{2}$ (from the curve for M), $M \simeq 0.5$ and $\eta = 0.9$ (worst cases). For larger values of M_0, the scale lengths for density and velocity variations are too short for ion-electron collisions to maintain T_i a constant.

To complete our study of viscous flow through a single mirror, we now consider the flow of a more viscous plasma. To do this we increase the value of λ_o/ℓ_c in Eqs. (7) and (16b). However, we are limited in the fluid theory to $\lambda \ll \ell_s$, where as before ℓ_s is a typical scale length for variations in n, v or A. Analogous to Eq. (8) this condition can be written in terms of our dimensionless variables as

$$\frac{\lambda_o}{\ell_c}\frac{\ell_c}{\ell_s}\frac{1}{\eta} \ll 1 \qquad (17)$$

For $M > \sqrt{m_e/m_i}$, this condition is less stringent than that of Eq. (8). To begin, we define ℓ_s in terms of $A(z)$ for which $\ell_s/\ell_c \simeq \frac{1}{2}$. For $\eta \simeq 1$, Eq. (17) then demands that $\lambda_o/\ell_c \ll \frac{1}{2}$. Choosing $\lambda_o/\ell_c = 0.1$ and $\nu_o' = 0$, we present two cases of purely subsonic flow in Fig. 6 as the curves labeled $M_o = 0.15$ and $M_o = 0.25$. We make the following comparisons to Fig. 5: (1) the points of velocity maxima and density minima are displaced farther downstream of the throat. (2) For the same value of M_o (for example, $M_o = 0.25$) the pressure (density) drop across the system is greater.

As M_o is increased, $M = 1$ first occurs at $\zeta \simeq 0.675$, presented by the curves labeled $M_o = 0.315$. Increasing M_o further results in a region of supersonic flow followed by a very slow transition back to subsonic flow, such as the case labeled $M_o = 0.325$. As M_o is increased still further, the region of supersonic flow increases until for $M_o = 0.331$ the flow downstream of the throat is entirely supersonic. Thus, we see that shock-like behavior vanishes in such a viscous plasma. As M_o is increased further, the position of the velocity maximum and density minimum moves out the exit. The curves for $M \simeq 1$ in the mirror throat are given by those labeled $M_o = 0.353$. Unlike the case $\lambda_o/\ell_c = 0.01$, no catastrophic behavior occurs for $M > 1$ in the throat. Referring back to Fig. 5, we notice that for $M \lesssim 1$ in the throat the velocity profiles exhibit inflection points near the throat.[6] However, for $M \gtrsim 1$ in the

---

[6] For $M = 1$ in the throat it can be shown using Eq. (16b) that this position is the inflection point.

throat, no such point exists and the profiles diverge. In the present case, however, the inflection point moves relatively slowly toward the exit as M is made greater than unity in the throat. Two examples are the curves labeled $M_o = 0.36$ and $M_o = 0.4$. In this sense the numerical solutions no longer demonstrate an obvious choking effect. We instead resort to intuition and a cursory study of the flow equation in asserting that choking still occurs for $M = 1$ in the throat, even with substantial viscosity, and that the profiles with $M > 1$ here are unphysical. Since shock fronts do not occur there is no need to initialize the integrations in the throat, where we specify $M = 1$ and vary $v'(.5)$. This is because we are able to generate all exist densities (pressures) down to that analogous to case (f) of Fig. 4 via the parameter M_o alone.

Although the curves are much smoother than those of Fig. 5, isothermy is found to be a poor assumption for all the cases shown in Fig. 6. Even for $M_o = 0.15$ where $\ell_s/\ell_c \simeq 0.6$, $M \simeq 0.3$ and $\eta \simeq 0.9$, the inequality (8) is badly violated. This is because λ_o/ℓ_c is a factor of ten larger than that of Fig. 5, resulting in relatively few ion-electron collisions. Finally we check if Eq. (17) is satisfied with ℓ_s/ℓ_c defined in terms of η and v, and taking into account the substantial decay of η along ζ (which lengthens the mean-free-path). Because ℓ_s/ℓ_c is large where η is small, Eq. (17) is still found to hold (although barely).

V. CONCLUSIONS

Comparing Figs. 4 and 5, we see that the flow of a nearly inviscid plasma through a magnetic mirror is very similar to fluid flow through a converging-diverging nozzle. However, the flow of a moderately viscous plasma is quite different, in that shock fronts do not develop. The fact that isothermy was a poor assumption does not hinder us in applying the results to subsonic multiple-mirror flow, in which shocks are excluded and the flow is usually slower. To see how this is done, consider a "half-system" with $z = 0$ corresponding to the midpoint of the multiple-mirror and $z = L$ an exit. In the limit $\lambda_o/\ell_c = 0$, Eqs. (15) give the solution for $a(\zeta)$ periodic. With $a(\zeta)$ given by Eq. (13), Fig. 3(a) represents an example of the profiles at any particular mirror of the device. As mentioned at that time, there is no change in the overall levels of density and velocity from mirror to mirror. However, the inclusion of viscosity results in an overall decrease in density (pressure) and an acceleration of the flow from mirror to mirror, as evident from the entirely subsonic profiles of Figs. 5 and 6. This effect is more dramatic with greater viscosity. For small pressure differences between the ends of our half-system, the flow will be as described. As the pressure difference is increased, sonic flow and subsequent choking will first occur in the exit mirror. In physical systems in which the exit pressure is low, a choked flow is a reasonable assumption, and $M = 1$ in the exit mirror throat becomes a "natural" boundary condition. Since we are not concerned with the flow beyond the exit mirror throat, shock fronts do not occur in the multiple-mirror. Furthermore, the flow is everywhere subsonic, adding to our justification in assuming isothermy. These observations will be made more quantitative in a forthcoming report.

REFERENCES

[1] Taylor, J. B., Wesson, J. A., Nuclear Fusion 5 (1965) 159.

[2] Trubnikov, B. A., "Particle Interactions in a Fully Ionized Plasma", in Reviews of Plasma Physics, Vol. 1, Consultants Bureau, New York, 1965.

[3] Shapiro, A. H., The Dynamics and Thermodynamics of Compressible Fluid Flow, Vol. 1, The Ronald Press, New York, 1953.

[4] Dawson, J. M., Uman, M. F., Nuclear Fusion 5 (1965) 242.

[5] Miller, G., Los Alamos Scientific Laboratory Report LA-7580-MS, Dec. 1978.

[6] Braginskii, S. I., "Transport Processes in a Plasma", in Reviews of Plasma Physics, Vol. 1, Consultants Bureau, New York, 1965.

[7] Hindmarsh, A. C., "Gear-Ordinary Differential Equation System Solver", UCID-30001 Rev. 3, Lawrence Livermore Laboratory, Dec. 1974.

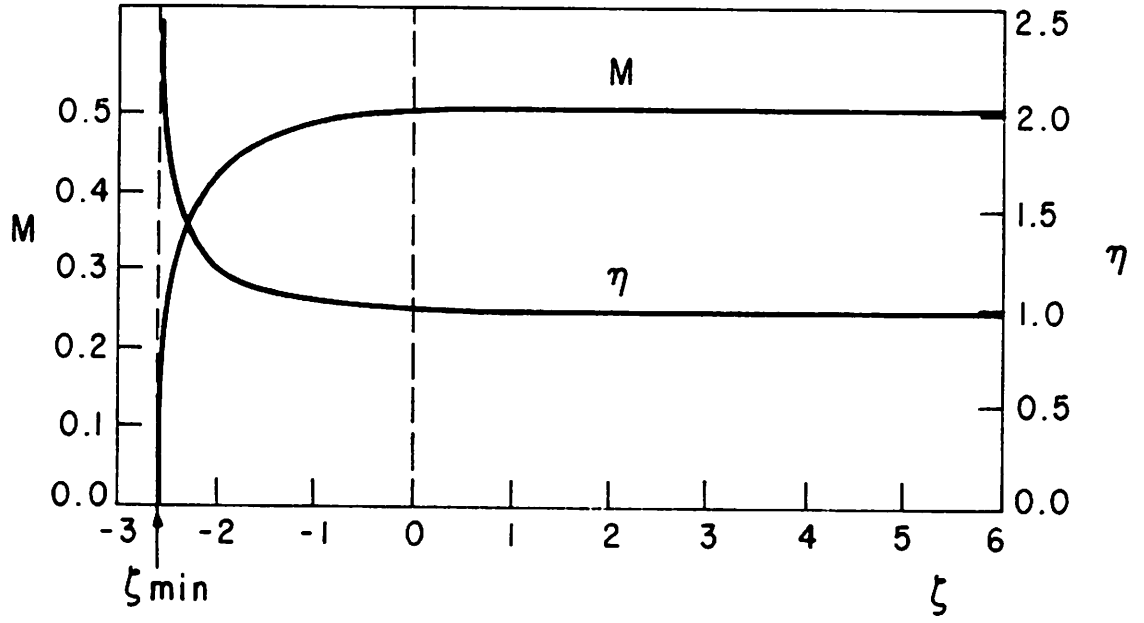

(a)

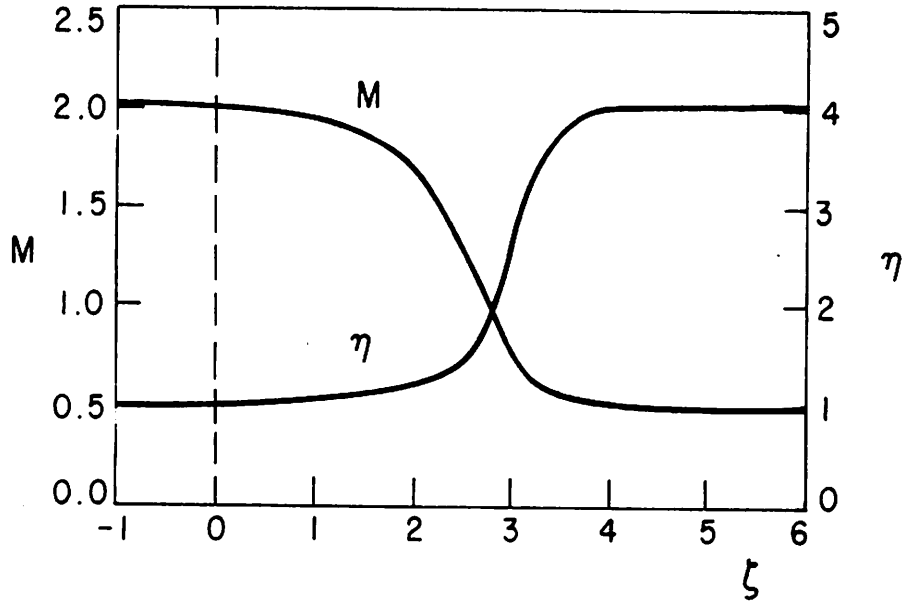

(b)

Fig. 1 Viscous flow along a uniform magnetic field ($\zeta = z/\lambda_o$)

(a) Subsonic flow ($M_o = 0.5$)

(b) Supersonic flow ($M_o = 2.0$)

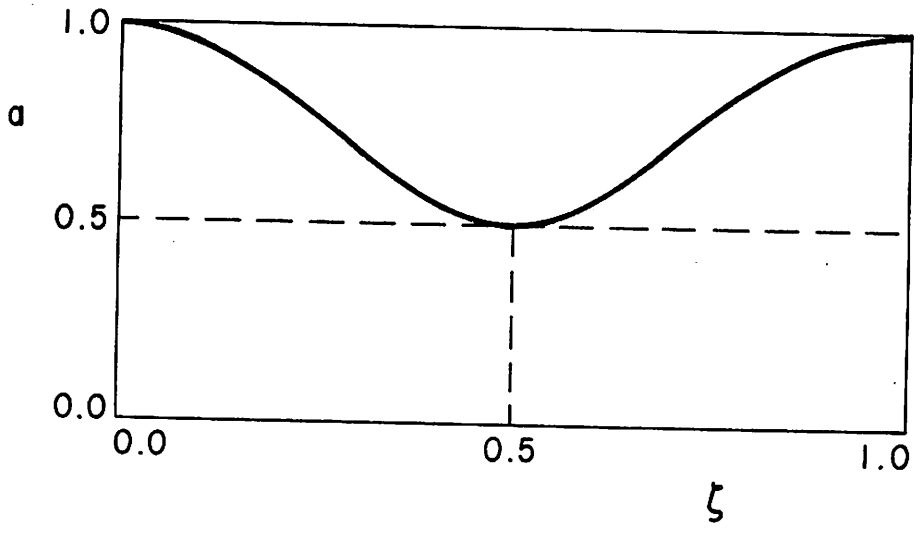

Fig. 2 The normalized plasma cross-section vs $\zeta = z/\ell_c$

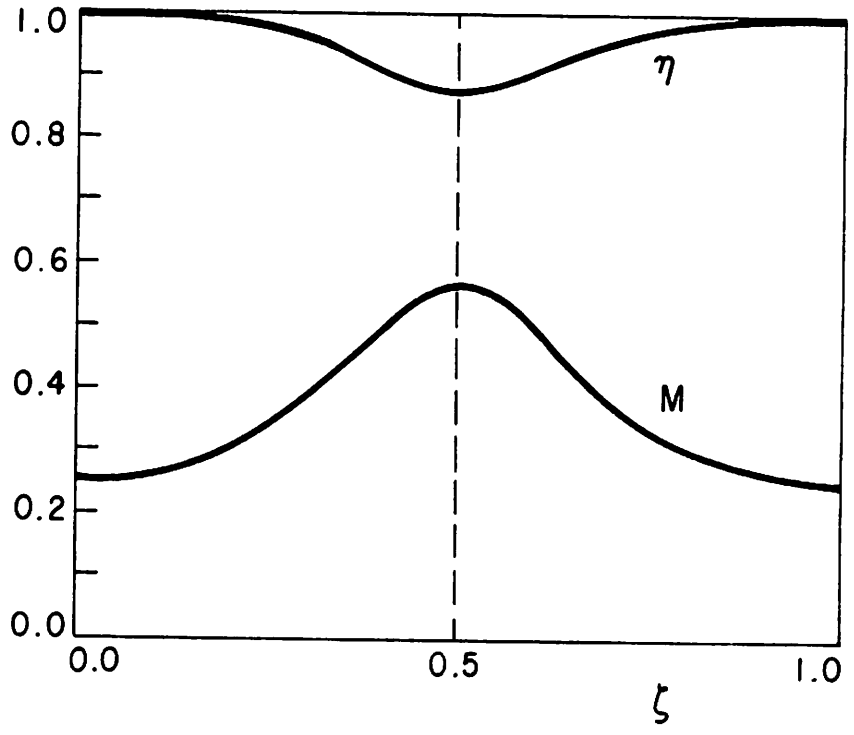

(a)

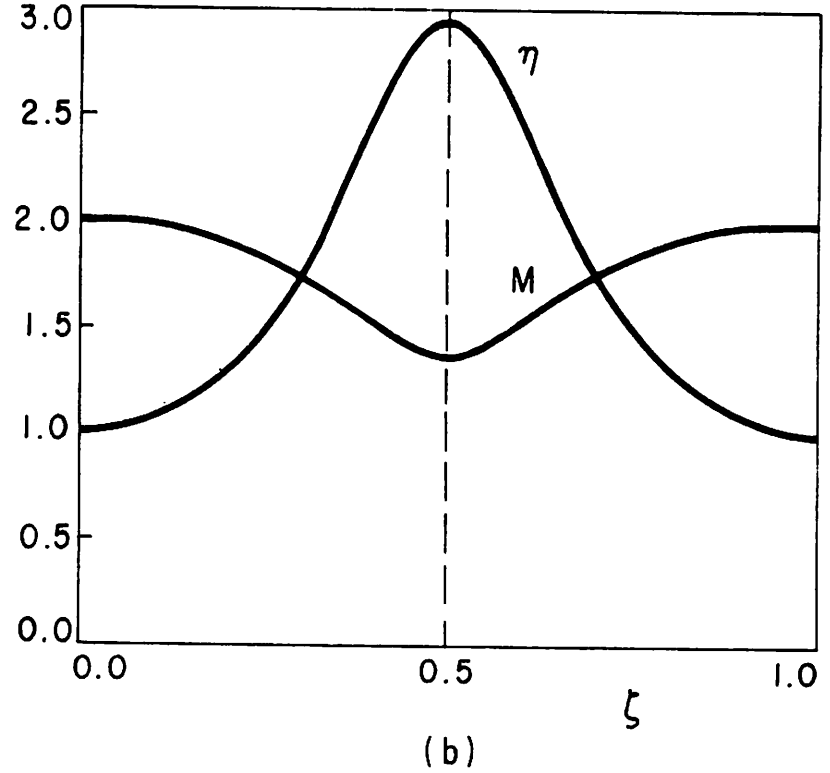

(b)

Fig. 3 Inviscid flow through a magnetic mirror ($\lambda_o/\ell_c = 0$)

(a) Subsonic flow ($M_o = 0.25$)

(b) Supersonic flow ($M_o = 2.0$)

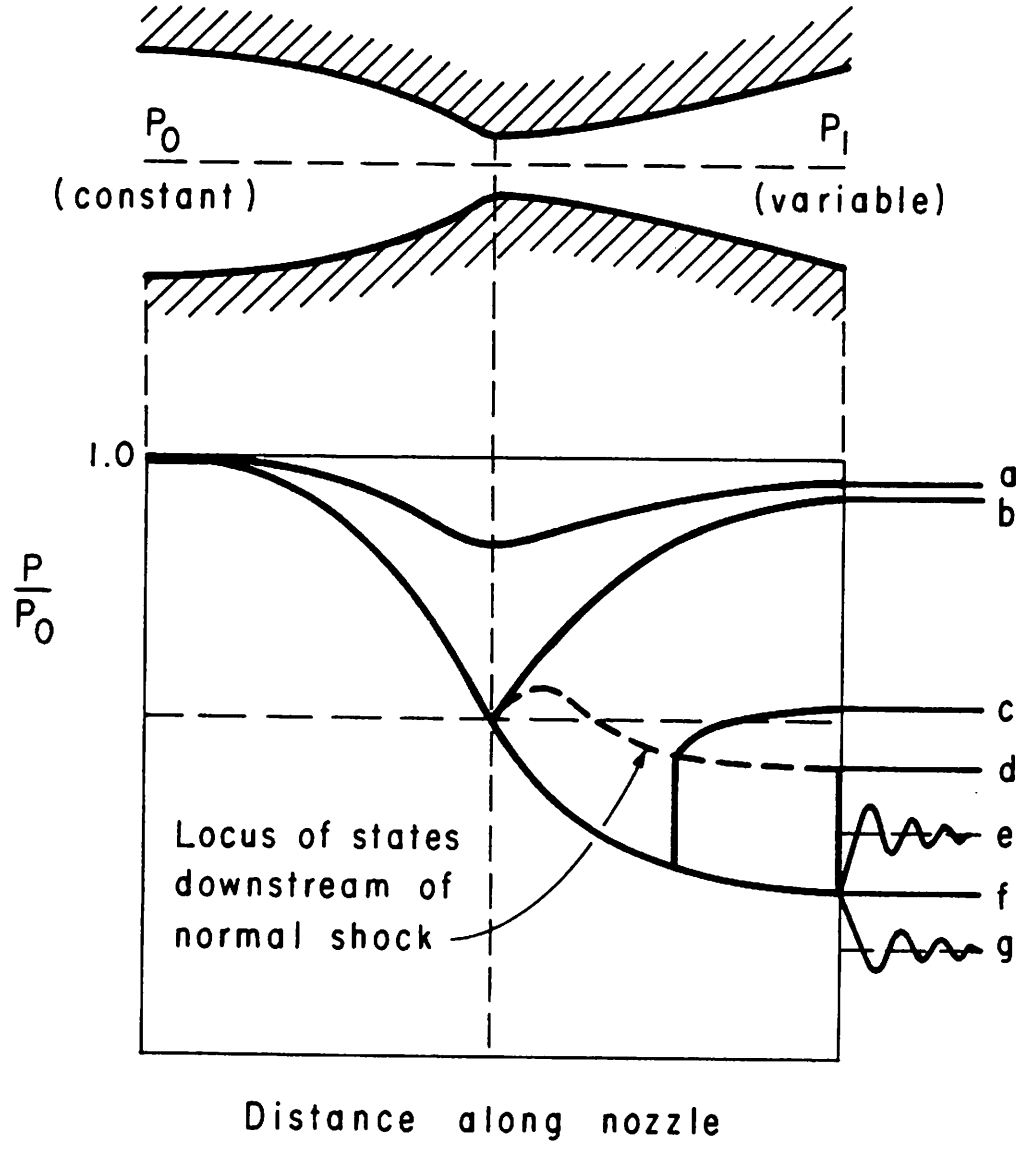

Fig. 4 Fluid flow through a converging-diverging nozzle

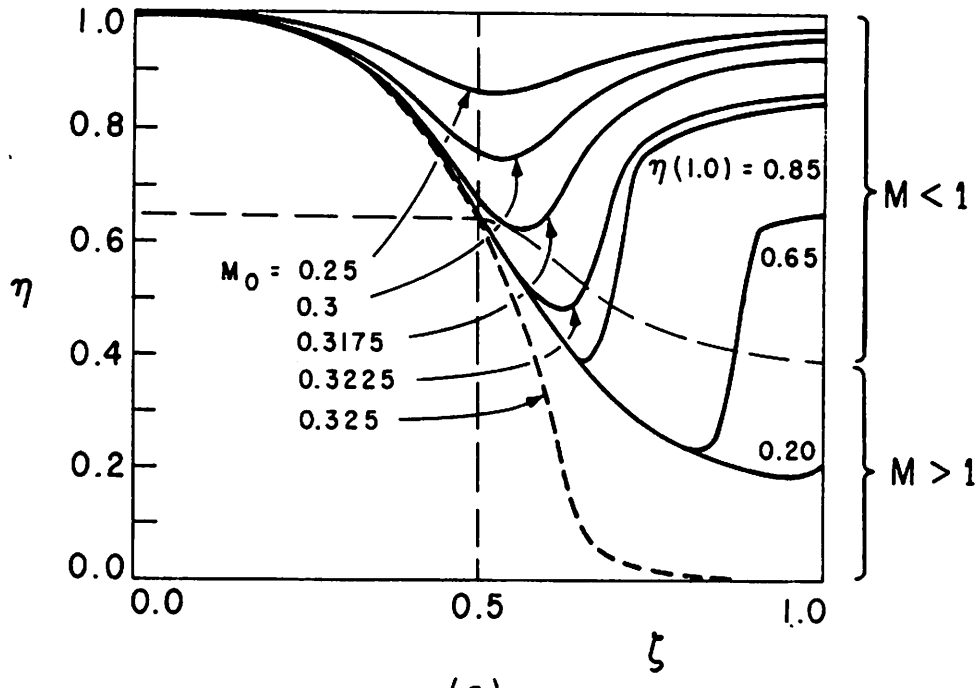

(a)

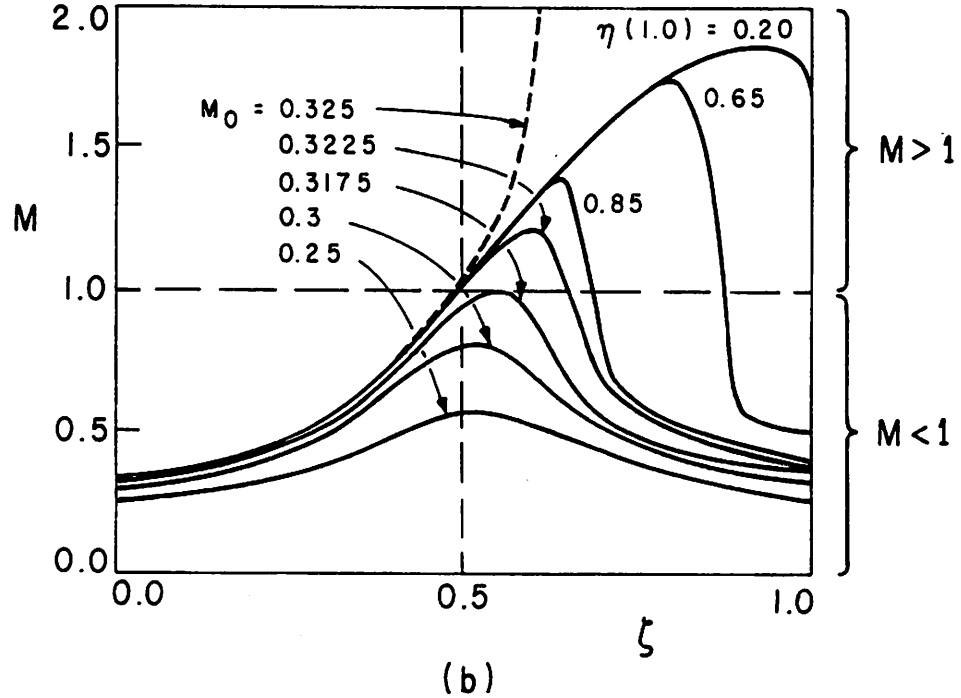

(b)

Fig. 5 Viscous flow through a magnetic mirror ($\lambda_o/\ell_c = 0.01$)

(a) normalized density vs $\zeta = z/\ell_c$

(b) Mach number vs $\zeta = z/\ell_c$

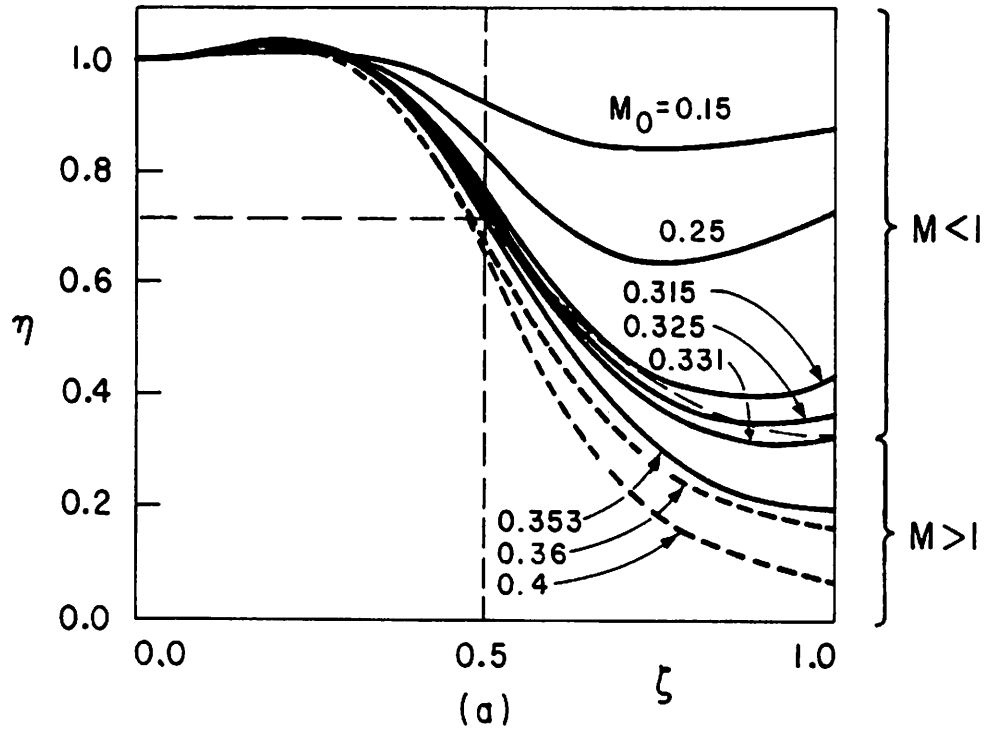

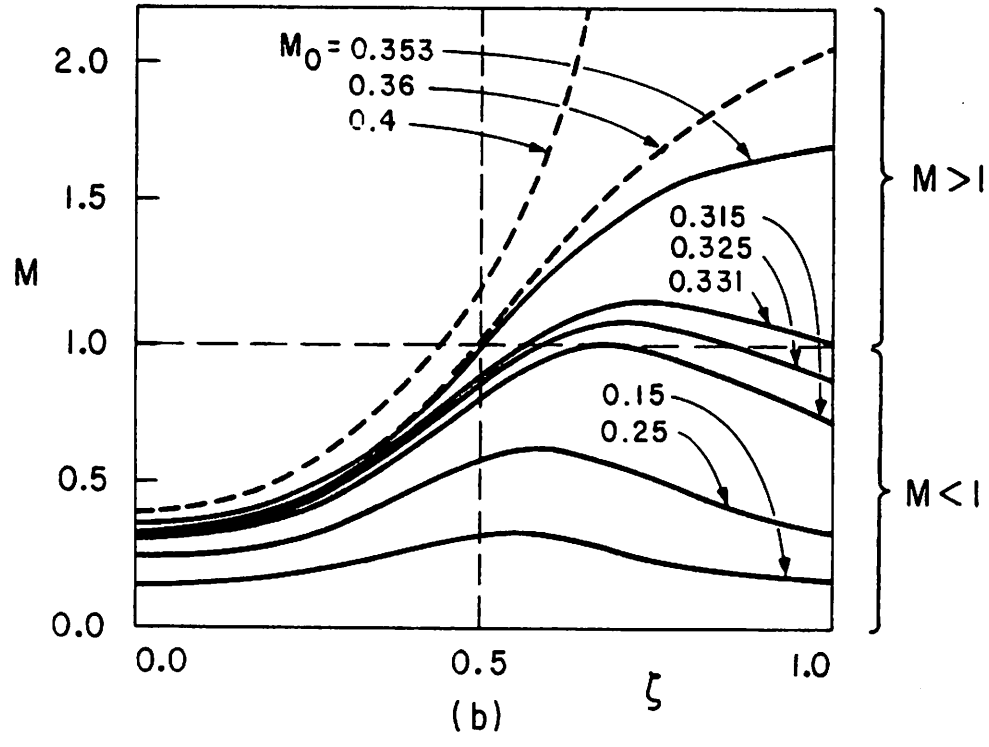

Fig. 6 Viscous flow through a magnetic mirror ($\lambda_o/\ell_c = 0.1$)

(a) normalized density vs $\zeta = z/\ell_c$

(b) Mach number vs $\zeta = z/\ell_c$